Northumbria Research Link

High order sliding mode control of a DC motor drive via a switched controlled multi-cellular converter

M. Djemaï[a*], K. Busawon[b] , K. Benmansour[c] and A. Marouf[a]

[a] Univ Lille Nord de France, F-59000 Lille, France, UVHC, LAMIH, F-59313 Valenciennes, France,
CNRS, FRE 3304, F-59313 Valenciennes, France, [*]Corresponding author
E-mail mohamed.djemai@univ-valenciennes.fr, alaa.marouf@gmail.com
[b] Northumbria University, School of Computing, Engineering and Information Sciences, Newcastle Upon Tyne,
UK. Phone: +44 (0)191 2273103, Fax: +44 (0) 2273684, email: krishna.busawon@unn.ac.uk
[c] University of Médéa, Electrical Engineering Department – Algeria. k_benmansour@yahoo.fr

Abstract: In this paper, we present a high order sliding mode controller of a DC motor drive connected to a multi-cellular converter. More specifically, we design a second order (super twisting) control algorithm for the speed regulation of a DC motor. For this, a switching control for the multi-cellular converter is derived in order to supply the correct reference value for the speed regulation. A practical implementation of the controller is realised using a laboratory set-up. The performance and the validity of the controller are shown experimentally.

Key words: Control of hybrid systems, sliding mode control, multi-cellular converter, super twisting algorithm.

1. Introduction

Control design techniques based on sliding modes have received considerable attention from researchers and engineers due to their intrinsic robustness (under certain conditions) and to the relative ease of implementation. Being discontinuous, this type of feedback is particularly well adapted for electric drive control. In effect, for technological reasons, the inputs for such systems are generally binary electrical signals; that is, they are naturally discontinuous. For more theoretical and practical descriptions the reader is invited to refer to some standard textbooks and articles on the subject, such as (Guldner et al., 1999), (Floquet at al., 2000), (Shyu and Lai, 2002), (Sira Ramirez and Ngai 2001), (Djemai and Barbot, 1999 and 2002), (Levant, 1998), (Emel'yanov et al., 1986), (Fridman and Levant, 1996), (Barbot, and Perruquetti, 2002), (Defoort et al., 2009) and (Laghrouch et al., 2007) just to mention a few. From a practical point of view, the control algorithms for electric drives are generally implemented via power converters using pulse width modulation (PWM).

The main objective of this work is to show that the multi-cellular converter (developed by LEEI Laboratory - actually LAPLACE Laboratory- (Meynard, and Foch, 1992)) is a typical example for which sliding mode control laws can be implemented (Utkin, 1992). In order to highlight the importance of using multi-cellular converters together with sliding modes, we shall only consider purely discontinuous control laws without using PWM algorithms. The serial multi-cellular converter enables the realisation of a safe assembly of power electronics components in cascade and operating in commutation. This new approach presents two additional advantages: the possibility of a modular construction and the possibility of using low cost and readily available components.

It is worth mentioning that in (Beaudesson, 2000), (Bethoux and Barbot, 2002) and (Bethoux, O., 2008) it was shown that, unlike standard converters, the serial multi-cellular converters have a longer life span due to the fact that, within a sampling period, there is only one switch that is operational at a time if the control is well defined. All these features render this new topology of power electronics very appealing.

In this paper, we shall use the advantages obtained by the efficient use of the multi-cellular converter as a power interface between a sliding mode type control and a DC motor drive. Specifically, a high order sliding mode (super twisting) controller is applied to the DC motor (DCM) connected to a multi-cellular converter. To start with, in the next section, the multi-cellular converter model is given followed by the regulation of the voltages across the capacitors' terminals in Section 3. Section 4 is devoted to the application of the high order sliding modes while the practical implementation and experimental results are given in Section 5. Finally, some conclusions are given.

2. Modelling of the multi-cellular converter

The multi-cellular converter is a variable structure system whose configuration changes during operation. It is characterized by the choice of a particular function and a switching or commutation logic. This choice enables the system to switch from one structure to another at every instant of time. Figure 1 depicts the topology of a serial multi-cellular converter with p autonomous commutation

*Corresponding author. Email: mohamed.djemai@univ-valenciennes.fr

cells (see Meynard and Foch, 1992) and (Meynard et al., 1997, and 2002).

Each cell is controlled by a binary function $u_k(t) \in \{0,1\}$. The association of the independent voltage source together with the converter and the load gives rise to a hybrid system. However, it must be noted that the converter itself is intrinsically hybrid due to the presence of switches and capacitors (V_{Ck} continuous variables).
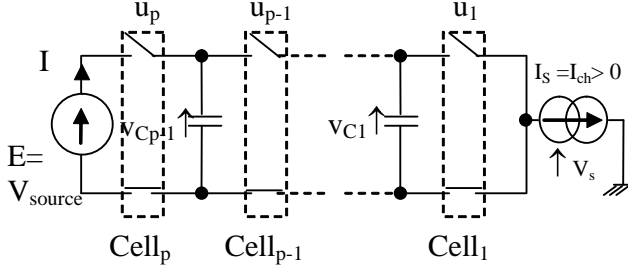

Figure 1. p cells serial multi-cellular converter

Each cell has to withstand the voltage $(V_{cell})_k$ with:

$$V_{cell_k} = (V_{C_k} - V_{C_{k-1}}) \qquad for \ k = 0,...,p$$

with $V_{C_0} = 0$, $V_{Cp} = V_{source} = E$ and p is the cells number.

On the other hand, the constraint of having an equal distribution of the voltage on each cell induces $(p-1)$ input references:

$$V_{C_k}^* = k \frac{V_{source}}{p} = k \frac{E}{p}; \quad for \ k = 1,...,p-1$$

In addition, the applied voltage to the load is given by:

$$V_s \ t = \sum_{k=1}^{n} u_k V_{cell_k} \qquad (1)$$

Let us define $(p+1)$ distinct voltage levels $(l/p)V_{source}$ with $\ell = 0,...,p$. The lth level is obtained by setting l cells among p to "1". Note that all the combinations are potentially required to realise a particular level. The voltages across the terminals of the capacitors are given by:

$$C_k \frac{dV_{C_k}}{dt} = I_s \ u_{k+1} - u_k \qquad \forall \ k = 1,...,p-1 \qquad (2)$$

Note that if the internal voltages V_{C_k} are randomly distributed between 0 and $V_E = \dfrac{(p-1)E}{p}$ (with nevertheless the constraint $V_{C_{k+1}} \geq V_{C_k}$ imposed by the anti-parallel diodes) then each control defines a different voltage level $V_s(t)$; which represent 2^n possibilities of combinations (here 8). If the converter is very close to its optimal state, which is essential for the protection of the p commutation cells, then all the control inputs $u = [u_1 \ldots u_p]^T$, such that

$$\sum_{k=1}^{p} u_k = \lambda$$

are equivalent for the output. This leads to (p+1) distinct values for the voltage $V_s(t)$. We therefore obtain (p+1) distinct levels: $\lambda \dfrac{V_{source}}{p} = \lambda \dfrac{E}{p}$ with $\lambda = 0,...,p$, is the position of the λth cell.

3. Regulation of voltage across the capacitors' terminals

The main aim of static power converters is to adapt the energy between the source (E, I) and the load V_s, I_s with the best efficiency possible so as to have minimum energy loss between the source and the load. This reduced energy loss is very important in the sense that it fixes the size, efficiency and reliability of the converter. As mentioned before, the serial multi-cellular converter permits to realise a safe serial assembly of components operating in commutation. In addition, it increases the degree of freedom for control and allows the use of fewer specific components. Currently, the implementation of the control is based on PWM of the ratio of duty cycles issued from the controller by regularly spaced triangular carriers. Generally, this permits to realise a simple and effective control of the converter and its load. However, in other cases, it was shown that the controller might become unstable for certain duty cycles (Benmansour, 2009), (Bethoux, 2008), (Carrere, 1996), (Gateau et al., 2002), (Meynard et al., 1992, 1997 and 2002).

Hence, it might be particularly interesting to make a converter with an arbitrary number of cells. First, because the choice of the number of semi-conductors components is largely determined by economical and technological constraints, as we have mentioned before. Next, because the serial multi-cellular converter has the ability of being reconfigured after a failure of one of its cells (Bethoux 2008). Therefore, the main problem is to be able to ensure the continuity of the operation of the static conversion whenever the control algorithm must handle p-1 cells.
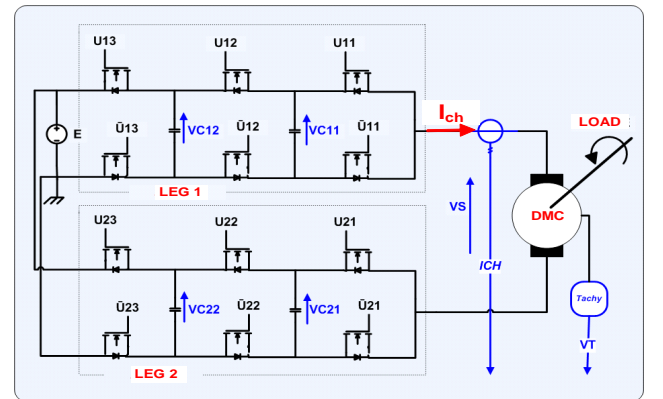

Figure 2. A DC Motor associated to 3 cells converter

The safe and proper functioning of the power converter directly depends on the suitable distribution of the voltages across each cell. That is why it is important to realise an internal regulation of the voltages across the terminals of the $(p-1)$ capacitors. Our structure (Figure 2) is made of two legs, each leg consisting of 3 cells

Thus, the state of the converter is determined by 6 control signals. Each leg can be controlled independently. Hence, it has to supply the necessary voltage in order to obtain the required value at the converter output. The dynamics of the converter is given by:

$$\dot{V}_{C11} = \frac{1}{C_{11}} \cdot \left[u_{12} - u_{11} \right] \cdot I_{ch}$$

$$\dot{V}_{C12} = \frac{1}{C_{12}} \cdot \left[u_{13} - u_{12} \right] \cdot I_{ch}$$

$$\dot{V}_{C21} = \frac{1}{C_{21}} \cdot \left[u_{22} - u_{21} \right] \cdot I_{ch}$$

$$\dot{V}_{C22} = \frac{1}{C_{22}} \cdot \left[u_{23} - u_{22} \right] \cdot I_{ch}$$

$$\dot{I}_{ch} = -\frac{R}{L} \cdot I_{ch} + \frac{1}{L} \cdot V_S - \frac{k}{L} \cdot \Omega$$

$$V_S = \left[\left(u_{11} - u_{12} \right) V_{C11} + \left(u_{12} - u_{13} \right) V_{C12} + u_{13}E \right]$$
$$- \left[\left(u_{21} - u_{22} \right) V_{C21} + \left(u_{23} - u_{22} \right) V_{C22} + u_{23}E \right]$$

One of the objectives of this work is to find a topology of the converter operating in four quadrants on the basis of a serial multi-cellular converter for the control of a DC motor using a single voltage source. In addition, this structure must allow magnetic braking. Finally, a control algorithm for the proposed structure is presented. The control algorithm is based on the redundancy of the states of the converter in order to obtain the different level of voltages at the converter output and at the terminals of the floating capacitors. This algorithm allows us to directly and independently use the different level of voltages of the converter.

The idea we tried was to set two multi-cellular converters in series as shown in Figure 2. This configuration is physically realisable. For this structure, we consider the following cases:

- The output voltage of the first leg is greater than that of the second leg: the current is therefore positive (the motor turns in the right direction)

- The output voltage of the first leg is less than that of the second leg: the current is therefore negative (the motor turns in the reverse direction)

- The output voltage of the first leg is equal to that of the second leg: breaking takes place.

4.1 Control Algorithm

We are now going to derive a direct control of the converter. This control must preserve the correct voltage level across the capacitors whatever the direction of the current (motor or generator mode). The characteristics of serial multi-cellular converters offer the possibility to adjust and to regulate the voltages across the floating capacitors by acting directly on the control signals of the latter. Firstly, it is imperative to know all the possible states as well as the values of the floating capacitor's voltages and the level of the output voltages of the converter for each state.

Table 1 gives the theoretical output voltage (V_s), the charge or discharge of the capacitors (C_{11}, C_{12}) as a function of the switching inputs (u_{11}, u_{12} and u_{13}) and the direction of the current (I_{ch+}, I_{ch-}).

The sign of the voltage variation at the terminals of the floating capacitors, ΔV_{Ck}, is described in the following manner: the 0 symbolises that the capacitors are not used, the (+) signifies that there is an increase in the capacitor charge, while the (-) corresponds to a decrease in the capacitor charge.

Now, let us focus on the control of the converter's switches. Obviously, owing to the structure of the converter, the switches of the same cell must be controlled in a complementary mode in order to avoid any short circuit of the voltage source. This structure consists of two legs, each leg having 3 cells. Hence, we have 6 control signals determining the state of the converter and the output voltage have seven levels:

$$\left\{ -E, -2\frac{E}{3}, -\frac{E}{3}, 0, \frac{E}{3}, \frac{2E}{3}, E \right\}.$$

As it can be seen in Table 1, each leg permits to generate four different voltage levels. In order to obtain a better precision during the control of the dc machine, we can generate ten (average) values of voltages from the four reference voltages $\left\{ 0, \frac{E}{3}, \frac{2E}{3}, E \right\}$. Consequently, the converter generates 19 voltage values. The voltage vector generated is

$$\left\{ 0, \frac{E}{9}, \frac{2E}{9}, \frac{E}{3}, \frac{4E}{9}, \frac{5E}{9}, \frac{2E}{3}, \frac{7E}{9}, \frac{8E}{9}, E \right\}$$

To generate these voltage values we divide the sampling period by three. Furthermore, knowing that we need at least three control cycles to maintain capacitor voltages around their reference values, we have again subdivided the chopping period by three. We therefore successively apply nine control actions during a chopping period. The choice of the control order sequence depends on the constraints: minimum commutation and using adjacent controls. In fact, due to this division by 9 of the chopping frequency, the switches operate at a classical chopping frequency of the converter, but the load sees a frequency that is 9 times the chopping frequency. This has the advantage of reducing the size of the filtering components at the output of the converter and thus shortening the tuning dynamics. At the same time, the chopping frequency of the switches can be reduced in order reduce the losses due to commutation. One must therefore find a trade off between losses and size of the converter, which goes hand in hand.

Remark 1 : This method is similar to an averaging procedure close to the PWM method but with respect to the 7 reference voltage of the multi-cellular converter instead of averaging with respect to 3 reference voltage for classical converter.

Thanks to Table 2, we can establish control law allowing maintaining voltages around their reference values by

assuming that the current is constant over a chopping period. As we can see, if we wish to generate a zero voltage, then the capacitors are not required. Similarly, the capacitors are not solicited in order to generate the voltage E or –E ; hence, only one control cycle is sufficient in order to regulate the voltages around their reference values.

However, if we wish to produce a voltage of value –E/3 or E/3 then one must use 3 different control cycles in order to regulate the capacitor's voltages. Similarly, in order to generate a voltage of -2E/3 and 2E/3 one would also need at least 3 cycles. Hence, according to Table 2, we can derive a control algorithm to maintain the capacitor reference voltages by considering the fact that the current is constant over one sampling period. The control law thus realised is straightforward and intuitive.

To illustrate the order according to which the controls are generated, let us consider the following examples.

Example 1: Generation of the voltage 2E/9 (if I_{ch} positive or negative)

To obtain this voltage level one must use the control (1, 2, 3, 4) of Table 1, in order to commute between 0 and E/3. Figure 2.1 depicts the order of the control sequence that was employed for that purpose, as well as the profile of the output voltage and the control signals. As it can be observed, the required voltage is obtained.
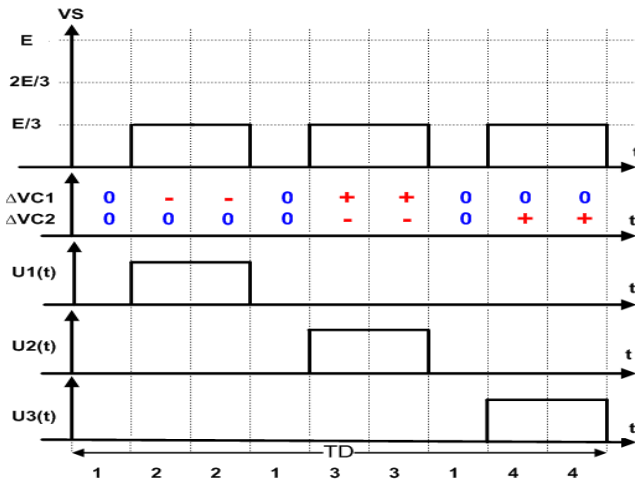

Figure 2.1 Control sequence for Vs=0 and E/3

Example 2: Generation of the voltage 4E/9 (if I_{ch} positive or negative)

To obtain this voltage level (***4E/9 (if I_{ch} positive or negative)***) one must use the control (2, 3, 4, 5, 6, and 7) in order to commute between E/3 and 2E/3. Figure 2.2 depicts the order of the control sequence that was employed for that purpose, as well as the profile of the output voltage and the control signals. Again, it can be observed, the required voltage is obtained.

Remark 2 : In the following section, we are going to use a second order sliding mode controller to control the DCM in order to obtain the desired reference speed (and current). In effect, the voltage which will be computed by the second order sliding mode algorithm will be utilised as a reference

signal at the output of the converter which the voltage $V_s(t)$ must follow in order to achieve the speed regulation.
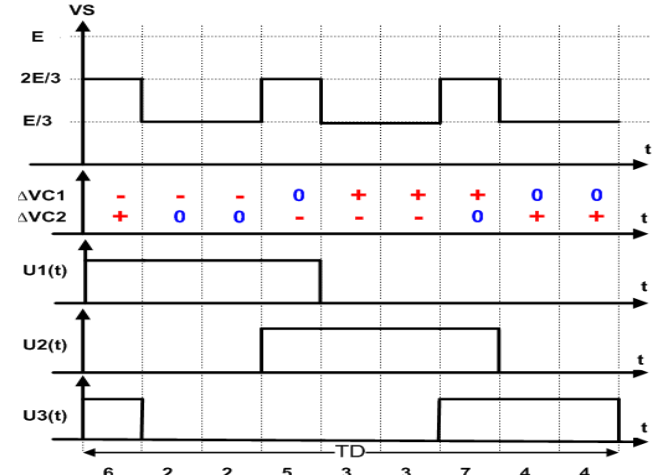

Figure 2.2 Control sequence for Vs=E/3 and 2E/3

The aim of the control algorithm that we have proposed is to find the correct switching combination so that the converter will supply the proper voltage reference; that is, as close as possible to that calculated by the sliding mode algorithm on the DCM.

4. High order sliding modes control

The synthesis of a sliding mode control is done in two steps: firstly, we determine a sliding surface $S(x)$ upon which the control objectives are realised. Next, we derive a control law in order to bring the state trajectory to this output and maintain it there at all time. The resulting control is discontinuous by nature. However, these algorithms did not generate an ideal sliding system and were likely to create local instabilities (chattering). In (Emel'yanov *et al.,* 1986), Emel'yanov *et al.,* proposed a new family of sliding mode called higher order sliding modes, (see also Levant et al., 1993). The main characteristics of high order sliding mode is that they act on the high order derivatives of the sliding surface while preserving all the advantages of 1st order sliding modes and reducing the chattering phenomenon while increasing the precision.

The order of the sliding mode characterise, in particular, the degree of continuity of the dynamics of the system around a neighbourhood of the surface and corresponds to the number of continuous derivatives of the variable to be constrained. For this, control algorithms capable of generating sliding mode at any order must be synthesised.

Consider a dynamic system described by (Barbot and Perruquetti 2002):

$$\dot{x} = f(x,u), \ S = S(x) \in \Re, \ u = U(x) \in \Re \qquad (3)$$

where: $x \in \Re^n$, f is a class C^1 function, u is the input function and the constraint S is a class C^2 function. By differentiating S with respect to time, *t*, we have:

$$\dot{S} = \frac{\partial}{\partial t} S(x) + \frac{\partial}{\partial x} S(x) f(x, u)$$

and

$$\ddot{S} = \frac{\partial}{\partial t} \dot{S}(t, x, u) + \frac{\partial}{\partial x} \dot{S}(t, x, u) f(t, x, u)$$
$$+ \frac{\partial}{\partial u} \dot{S}(t, x, u) \dot{u}(t) \qquad (4)$$

The aim is to obtain a control u such that the constraint $S=0$ is verified and $S = \dot{S} = 0$ is maintained.

The proof of the existence of a solution has been established under the following conditions:

• The control u is a bounded function $|u| \leq U_M$; $\forall t$.

• Suppose there exists $u_1 \in [0,1]$ such that $\forall u; |u(t)| > u_1, \forall t$ then, $S(t).u((t)>0$ for a finite set of t.

• There exist positive constants S_0, K_m, K_M, u_0 with $u_0 < U_M$ such that: if $|S(t, x)| < S_0$ then

$$0 < K_m \leq \frac{\partial}{\partial u} \dot{S}(t, x, u) \leq K_M \qquad \forall u \qquad (5)$$

The set $t, x, u : |S(t, x)| < S_0$ is the linear region.

• There exists a positive constant Φ in the linear region such that :

$$\left| \frac{\partial}{\partial t} \dot{S}(x, u) + \frac{\partial}{\partial x} \dot{S}(x, u) f(x, u) \right| \leq \Phi \qquad (6)$$

Then, there exists a control law $u = \varphi(S, \dot{S})$ which allows to reach the surface $S = x : S = \dot{S} = 0$ in finite time; which is represented by the origin point $(0, 0)$ in the phase plane $(S, \dot{S})$.

One can find several examples of algorithms ensuring a second order sliding mode in the literature, for example see (Levant 1998), (Fridman and Levant 1996), (Levant et al 1993), (Barbot and Perruquetti, 2002), (Djemaï and Barbot, 2002) and (Djemai at al., 1999) just to mention a few. Hereafter, the ‹‹Super-Twisting›› algorithm is recalled:

$$u(t) = u_1(t) + u_2(t)$$

$$\dot{u}_1 = \begin{cases} -u & \text{if} & |u| > U_M \\ -\alpha \cdot sign(S) & \text{if} & |u| \leq U_M \end{cases} \qquad (7)$$

$$u_2 = \begin{cases} -\lambda \cdot |S_0|^\rho \cdot sign(S) & \text{if} & |S| > S_0 \\ -\lambda \cdot |S|^\rho \cdot sign(S) & \text{if} & |S| \leq S_0 \end{cases}$$

with α, λ, ρ verifying the following inequality:

$$\alpha > \frac{\phi}{K_m}$$
$$\lambda^2 \geq \frac{4\phi}{K_m^2} \cdot \frac{K_M (\alpha + \phi)}{K_m (\alpha - \phi)} \qquad (8)$$

with $0 < \rho \leq 0.5$.

The main advantage of this algorithm is that it does not require the knowledge of the sign of the derivative of S. In effect, it is very difficult to measure the sign of the derivative of S due to the presence of noise.

4.2 Application to the DCM speed control

The main objective of the proposed super twisting control algorithm is to follow the reference speed trajectory. This control only requires the measurement of the engine's rotating speed. An exact robust differentiator will be developed to estimate the acceleration of the engine.
The DCM model can be written as follows:

$$\begin{cases} \dfrac{d\Omega}{dt} = \dfrac{k}{J} \cdot I - \dfrac{1}{J} \cdot C_r \\ \dfrac{dI}{dt} = \dfrac{1}{L} \cdot U - \dfrac{R}{L} \cdot I - \dfrac{k}{L} \cdot \Omega \end{cases} \qquad (9)$$

where U, I, L and R are respectively the voltage, the current, the inductance and the coil resistance, Ω represents the motor shaft angular speed, C_r the torque and k, J represent respectively the torque constant, the total inertia of the DC Motor. Here, the use of a second order sliding modes control law enables to assign the angular velocity ω to the desired value, in finite time. Let e be the difference between the current engine speed and the reference speed: $e(t) = \Omega(t) - \Omega_{ref}(t)$.

Generally, the most common choice adopted for the function S is a linear combination between the error e and a certain number of its derivatives with respect to time (depending on the relative degree of the system).

Consider the following sliding surface:

$$S = \frac{d}{dt} e(t) + c \cdot e(t)$$
$$= \frac{d}{dt} \left(\Omega(t) - \Omega_{ref}(t) \right) + c \cdot \left(\Omega(t) - \Omega_{ref}(t) \right) \tag{10}$$

One can see that speed of convergence to the surface $S=0$ depends on the constant c; that is,

$$\exists \ t \geq t_1 : S(t) = 0 \Rightarrow e(t) = e(t_1) . \exp\left(-c \cdot (t - t_1)\right) \quad t \geq t_1$$

To calculate the parameters α, λ of the "Super-Twisting" control law, one must calculate the second derivative of S and then choose the constants Φ, K_m, K_M such as the sliding conditions are verified.

Let us assume, for the time being, that the shaft acceleration of the motor is available. By differentiating S once, and using (9), we have:

$$\dot{S} = \frac{k}{JL}\left[U - k\Omega + (cL - R)I - \frac{cL}{k}C_r - \frac{L}{k}\dot{C}_r - \frac{cJL}{k}\dot{\Omega}_{ref} - \frac{JL}{k}\ddot{\Omega}_{ref} \right]$$
$$= \frac{k}{JL}U + g(t) \tag{11}$$

with:

$$g(t) = -k\Omega + (cL - R)I - \frac{cL}{k}C_r - \frac{L}{k}\dot{C}_r - \frac{cJL}{k}\dot{\Omega}_{ref} - \frac{JL}{k}\ddot{\Omega}_{ref} \tag{12}$$

$$\ddot{S} = \frac{k}{JL}\left[\dot{U} + \dot{g}(t) \right] \tag{13}$$

By identifying (13) with (5), (6), we obtain:

$$\left| \dot{g}(t) \right| \leq \Phi; \quad and \quad K_m \leq \frac{K}{JL} \leq K_M \tag{14}$$

Now, it only remain to calculate the upper bound of $\left| \dot{g}(t) \right|$; i.e Φ.

The coefficients α, λ, ρ are calculated using (8).

Acceleration estimation

The proposed controller requires the real time computation of the shaft angular acceleration of the engine. As mentioned before, the speed signal is the only measured variable. As a result, the acceleration must be estimated from the speed measurement. To control the output voltage of the converter, an observer for the voltage across the capacitors could be used. This will allow us to drive the voltage across each floating capacitors. The design of an observer is not considered here because it requires the exact knowledge of the motor parameters. As a result, the robustness of the controller might be lost. Consequently, the best choice is to use a real time differentiator. The required differentiator must be exact and robust with respect to the possible measurement errors and input noises and have finite convergence time (Levant, 1998), (Saadaoui et al., 2006).

Consider a signal $x(t)$ measured in real time such that:

$$\left| \dot{x}(t) \right| \leq X \qquad X > 0, z(0) = x(0) \ et \ w(0) = 0$$
$$h = -\lambda_1 \left| z - x \right|^{0.5} \cdot sign(z - x) + w$$
$$\dot{w} = -\lambda_2 \cdot sign(z - x) \tag{15}$$
$$\dot{z} = h$$

with λ_1, λ_2 verifying the following inequalities:

$$\lambda_1 > X \qquad \lambda_2 \geq 2 \cdot \sqrt{X \cdot \frac{\lambda_1 + X}{\lambda_1 - X}} \tag{16}$$

One can show that, after a finite time,
$$h(t) = \dot{x}(t) \tag{17}$$

In fact, the differentiating circuit equations can be viewed as a «Super-Twisting» controller, converging in final time to the surface

$$\varepsilon = \left\{ x : \varepsilon(t) = z(t) - x(t) = \dot{\varepsilon}(t) = h(t) - \dot{x}(t) = 0 \right\}$$

The discretization of the differentiator is obtained using the Euler's method:

$$h_k = -\lambda_1 \left| z_k - x_k \right|^{0.5} \cdot sign(z_k - x_k) + w_k$$
$$w_k = w_{k-1} - T_e \cdot \lambda_2 \cdot sign(z_{k-1} - x_{k-1}) \tag{18}$$
$$z_k = z_{k-1} + T_e \cdot h_{k-1}$$

for $k=0,1,2$; with $z(0) = x(0) = z_0 = x_0 = 0$ and T_e is the sampling period.

The proposed acceleration estimator, which is made of a second order sliding mode differentiator, necessitates the computation of two positive constants satisfying inequality (16). To determine these values, the acceleration must be bounded by using the maximum voltage and current of the components.

Remark 3 : The *sign* function produces high frequency oscillations close to the sliding surface.

In fact, the ideal condition $S = \dot{S} = 0$ cannot really be attained in the real system; it oscillates around zero and therefore generates high frequency commutations. To reduce the commutation frequency, the *sign* function is substituted by the hysteresis function (as depicted in Figure 3):

$$hys(S) = \begin{cases} +1 & if \quad S > \Delta \\ -1 & if \quad S < -\Delta \end{cases} \tag{19}$$
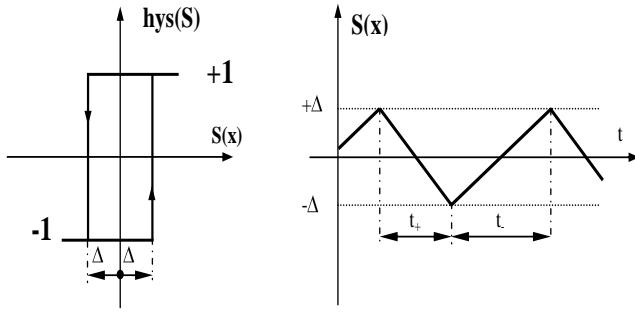
Fig. 3 Commutation law with hysteresis

5. Practical implementation and experimental results

In this section, the experimental set-up employed to demonstrate the performances of the proposed controller and to evaluate its feasibility is presented. The experimental set-up is a laboratory model of low power, designed for pedagogic (or education) and research applications. Figure 4 shows a block diagram of the test rig and the four different parts of the model:
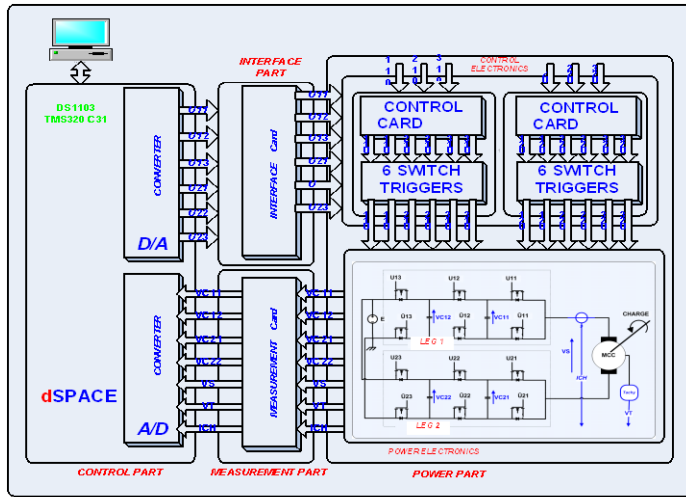

Fig. 4 Block diagram of the test bench

- The power part includes:
  - A 3 cells multi cellular converter (two valve legs), switches and capacitors.
  - Control equipment and triggers.
  - The load of DCM type.
- The measurement part is composed of voltage sensors – to measure the voltage across the floating capacitors - and the tachometer voltage, and a current sensor for the load current.
- The control part is composed of a control electronic board DS1103, based on a floating point DSP (TMS320C31) of 50MHZ working frequency. Its principal interest is to allow the design of the main part of the control algorithm using block diagrams; by using the Matlab-Simulink software. The Real Time Workshop tool is employed in order to provide a rapid and effective way to translate the simulations models into C language; by using an automatic procedure for coding, compilation, link edition and executable files downloaded on the DSP processor.
- The interface part sets the optical isolation and the outputs protection of dSPACE.

A three cells converter is used and its parameters are: $C_1 = C_2 = 40 \mu F / 400V$, $F_d = 1Khz$, $T_{ech} = 100 \mu s$, $E = 30V$. The DC motor parameters (Parvex Alsthom MC 17H) are: Nominal power: 375w, and Nominal speed: 3000 tr/min, $R = 1.8\Omega$, $J = 79 \cdot 10^{-5} \cdot kg \cdot m^2$, $K_T = 0.286 Nm / A$. The tachometer parameters, mounted directly on the shaft, are: $K = 20$ $V / 1000 \min^{-1}$, $J = 14.5 \cdot 10^{-5} \cdot kg \cdot m^2$.

La mise en place de la commande et de l'observateur, en pratique et leur implémentation, a nécessité la discrétisation du modèle avec un choix judicieux de la période d'échantillonnage et un modèle partiellement moyenné.

During the various tests the chopping frequency was set to $F_d = 2$ KHZ, the sampling period was $T_{eh} = 100$ µs, the sign functions have been replaced by a hysteresis function as in (19). In fact, a better behaviour is experimentally obtained using this function. The tuning of the control coefficients is done via a trade off between accuracy, response time and chattering attenuation. Figure 5 shows the speed response with respect to its relative value. As it can be seen, the speed converges to its reference trajectory. Figure 6 shows the output voltage control by Super-Twisting algorithm and the voltage of the converter output.

Figure 7 shows the evolution of the voltage across the floating capacitors. In order reduce the fluctuations of the voltages the value of the capacitors can be increased. Finally, Figure 8 a) and b) shows the speed response when a step is applied. A good converging performance can be observed.
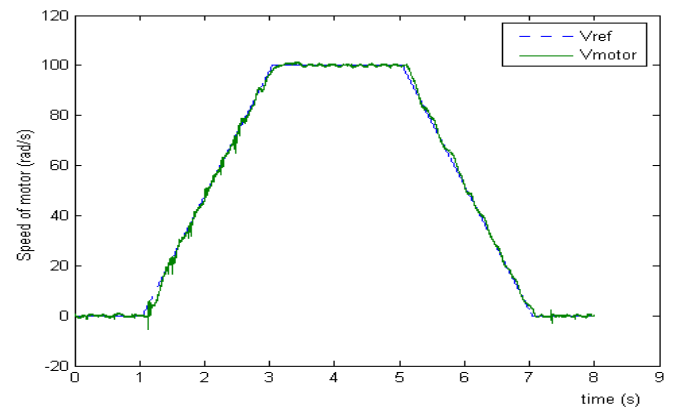

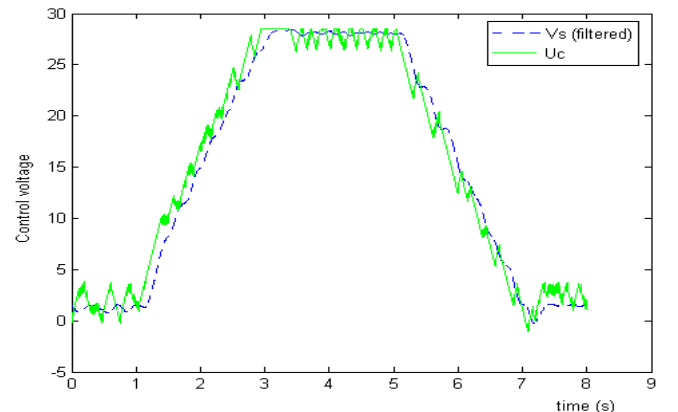Fig. 5 Response time of speed of the motor with its reference value

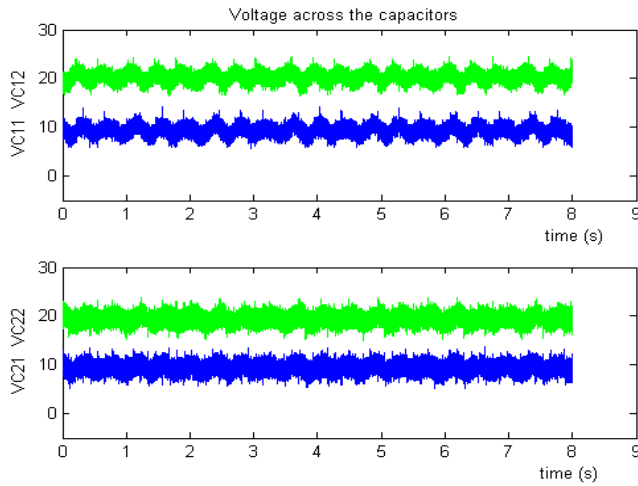Fig. 6 Control and converter output voltage

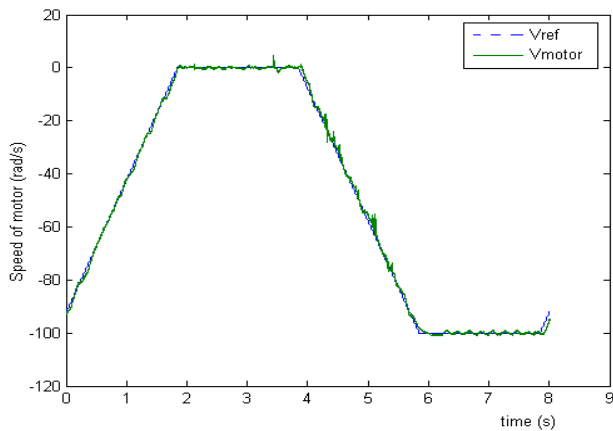Fig. 7 Evolution of the voltage across the floating capacitors

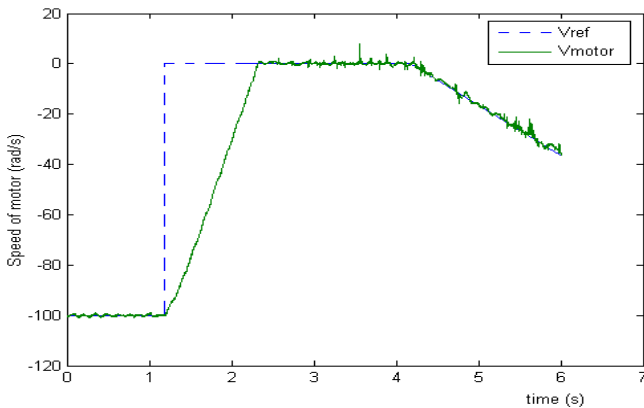Fig. 8 a): Performance of the system with a negative speed

Fig. 8 b) Performance of the system with a negative speed

Remark 4 : Il est a noté que les deux commandes (celle du convertisseur et celle du moteur) sont liées. La commande obtenue pour le moteur constitue une référence pour la commande de la partie puissance (le convertisseur multicellulaire).

De plus, la machine à CC (DC-Motor) est alimenté par le convertisseur multicellulaire, la machine a CC est naturellement réversible (fonctionnement en quatre quadrant) (moteur et freinage), cette réversibilité est liée directement au convertisseur d'où le choix de cette structure permettant un tel fonctionnement.

6. Conclusion

In this paper, a super twisting control algorithm for the speed control of a DCM connected to a switched controlled multi-cellular converter has been proposed. A detailed description of the switching control algorithm for the multi-cellular converter has been presented. It is shown that the multi-cellular converter is a promising and suitable power system interface for the implementation of sliding mode control laws. Experimental results have allowed us to highlight the advantages and the performances of such a control strategy.

References

Barbot, J.P. and Perruquetti, W., *Sliding mode control in engineering,* Marcel Dekker, 2002.

Beaudesson, P. *Sûreté de fonctionnement, reconfiguration et marches dégradées des convertisseurs multiniveaux à IGBT.*, PhD. Thesis, Institut National Polytechnique de Toulouse, octobre 2000.

Benmansour, K., Réalisation d'un banc d'essai pour la Commande et l'Observation des Convertisseurs Multicellulaires Série: Approche Hybride, PhD Thesis, Université de Cergy, Juin, 2009.

Bethoux, O. Barbot, J.P., Multi-cell chopper direct control law preserving optimal limit cycles. *Proceedings of CCA,* Glasgow, 2002.

O. Bethoux, J. Barbot, M. Hilairet, "Multicell actuator based on a sliding mode control", "European Physical Journal-Applied Physics", Vol. 43, 2008, pp. 217-223

Bethoux, O., and J.P. Barbot, "Multi-cell chopper direct control law preserving optimal limit cycles", in *Proceedings of CCA*, Glasgow, 2002.

Carrere, P. « Etude et réalisation des convertisseurs multicellulaires série à IGBT» Thèse de Doctorat, Thesis, Institut National Polytechnique de Toulouse, (INPT), 1996.

Defoort M., Noellet F., Floquet T., Perruquetti W. A third order sliding mode controller for a stepper motor. IEEE Transactions on Industrial Electronics, 56 (9), pp. 3337-3346, 2009

Djemaï, M., and Barbot, J.P. Smooth Manifolds and High Order Sliding Mode Control. *Proceedings of IEEE Conference on Decision and Control,* 2002.

Djemaï, M, J.P. Barbot and T. Boukhobza ``*Some comments on higher order sliding modes utilities*'' European Control Conference, **1999.**

Emel'yanov, S.V., Korovin L.V. and Levantovsky, A. Higher order sliding mode in the binary control system. *Soviet Physics,* vol. 31 – n°4, pp 291-293, 1986.

Floquet, T., Barbot J.P. and Perruquetti, W. Second order sliding mode control of induction motor. *Proc. Of IEEE Conf. on Decision and Control*, Australia, 2000.

Fridman, L., and A. Levant, "Sliding modes higher order as a natural phenomenon in control theory," In F. Garafalo, L. Glielmo (Eds.), Robust control via variable structure & Lyapunov Techniques- Lecture Notes in Control and Information Science; 217, Springer Verlag, London, 107-133, 1996.

Gateau, G. Fadel, M. Maussion, P. Bensaid, R. Meynard, T.A «Multicell Converters: Active Control and Observationof Flying-Capacitor Voltages». IEEE transaction on industrial electronics, V.49, N°5, pp 998_1008, 2002.

Guldner, J., Utkin, V.I and Shi, J. *Sliding mode control in electromechanical systems*. Taylor & Francis, 1999.

Laghrouche. S, Plestan. F., and Glumineau A. Higher order sliding mode control based on integral sliding mode, *Automatica 43 (2007) 531 – 537*

Levant, A., Robust Exact Differentiation via sliding mode technique, *Automatica,* Vol. 34, No. 3, pp. 379–384, 1998.

Levant, A., S.V. Emel'yanov and S.K. Korovin "Higher order Sliding mode in control system," Differential equations, 29(11): 1627-1934, 1993

Meynard, T., and Foch, H., « Dispositif de conversion d'energie electrique, à semi-conducteur » French patent N°91,09582 du 25 juillet 1991, dépôt international PCT (Europe, Japon, USA, Canada), No. 92, 00652 du 8 juillet 1992.

Meynard, T. and Foch, H., « Milti-level choppers for high voltage applications » EPE Journal, V.1 N°.1, 1992.

Meynard, T., M. Fadel, N. Aouda «Modeling of Milti-level converters» IEEE Transaction on Industrial Electronics, V.44, N°.3, pp.356-364, 1997.

Meynard, T., H. Foch, F. Forest, Ch. Turpin, F. Richardeau, L. Delmas, G.Gateau, E.Lefeuvre « Miltcell converters: Derived topologies » IEEE transactions on Industrial Electronics, V.49, N°.5, pp.978-987, Special Issue on Multilevel converters, Octobre 2002.

Shyu, K.K. and Lai, C.K. Incremental motion control of synchronous reluctance motor via multi-segment sliding mode conrol method. *IEEE Transactions. On Control systems Technology*, vol. 10 , No. 2, 2002.

Sira-Ramirez, H. and Ngai, A. Static and dynamic sliding mode control schemes for permanent magnet stepper motor. *Int. Journal of Control*, Vol. 74, No. 2, pp. 103-117, 2001.

Saadaoui, H., N. Manamanni, M. Djemaï, J.P. Barbot and T. Floquet, *Exact differentiation and sliding mode observers for switched Lagrangian systems*, in Nonlinear Analysis: Theory, Methods & Applications, Ed. Elsivier, Vol.65, (5), **pp.** 1050-1069, **2006**.

Tachon, O, « Commande découplante linéaire des convertisseurs multicellulaires série » Thèse de Doctorat, Thesis, Institut National Polytechnique de Toulouse, (INPT), 1998.

Utkin, V.I. *Sliding mode in control and optimization,* Springer Verlag, 1992.

Appendix: **Notations**

$V_{source} = E$: Source voltage

V_{cellk} = Voltage across k^{th} Cell.

C_k : k^{th} Capacitor

V_{ck} : Voltage across capacitor C_k

V_s : Load Voltage

I_s : Load Current

p : Number of cells (p-1: number of capacitors)

R : armature resistance of the DCM

k : back-emf coefficient

J : Moment of inertia

ω_n : nominal speed of the DCM

Appendix : The presentation of test bench

In this appendix, the different parts of the test-rig are presented on which the control algorithms have been tested and validated. The Figures A.1 and A.2 show the different test-rig parts. There is a dissociation of the control and power parts, which allowed the development of other control structures while using the same power system structure. It has to be mentioned that the reliability and the simplicity of the dSPACE DSP system and its processing power facilitated considerably the setting up of the rig.
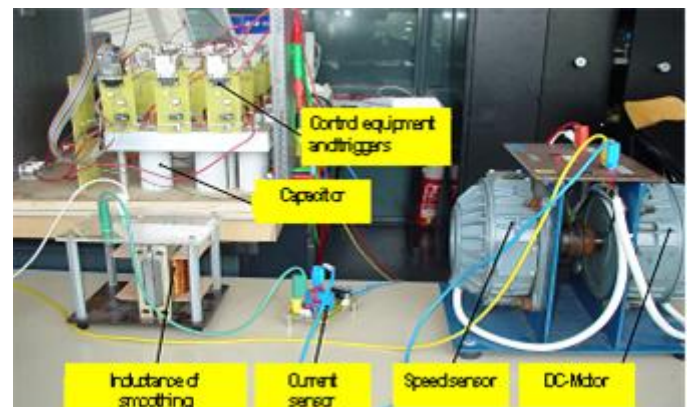
Fig.A.1 The engine converter and smoothing inductor unit.
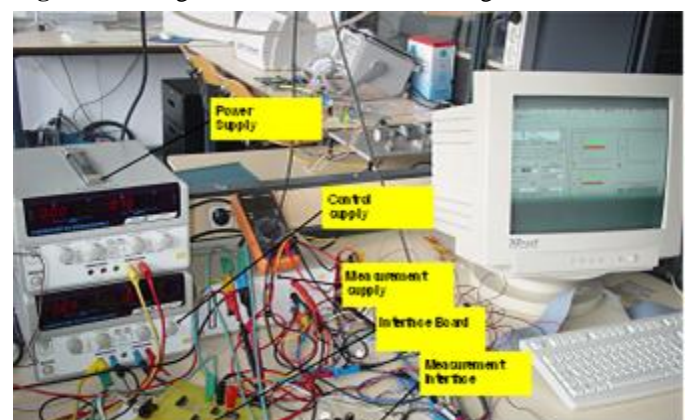
Fig A.2: *Measurement board and interface with power supply*

machine.

Mohamed DJEMAI, is actually professor at University of Valenciennes (France). He is with « Laboratoire d'Automatique, de Mécanique et d'Informatique industrielles et Humaines (LAMIH–Laboratory, CNRS). He received his PhD degree in automatics from Paris XI University (France) in 1996 and HDR in 2005. Actually, his main reasearch activities deal with nonlinear systems in continuous time and under sampling, sliding mode mode control and observrs, fault detection and residual generation and Hybride Dynamical systems. The domains of applications are robotics and electrical

N°	Control Switchs			Ic12		Ic22		ΔV_{C12}		ΔV_{C11}		Vs1
	u11	u12	u13	Current		Current		Current		Current		
				P	N	P	N	P	N	P	N	
1	0	0	0	0	0	0	0	0	0	0	0	0
2	1	0	0	0	0	Ich-	Ich+	0	0	(-)	(+)	E/3
3	0	1	0	Ich-	Ich+	Ich+	Ich-	(-)	(+)	(+)	(-)	E/3
4	0	0	1	Ich+	Ich-	0	0	(+)	(-)	0	0	E/3
5	1	1	0	Ich-	Ich+	0	0	(-)	(+)	0	0	2E/3
6	1	0	1	Ich+	Ich-	Ich-	Ich+	(+)	(-)	(-)	(+)	2E/3
7	0	1	1	0	0	Ich+	Ich-	0	0	(+)		2E/3
8	1	1	1	0	0	0	0	0	0	0	0	E

Table.1 Main features of one Leg of the converter with 3 cells

Vs	P11	P12	P13	P14	P15	P16	P17	P18	P19	P21	P22	P23	P24	P25	P26	P27	P28	P29
E	8	8	8	8	8	8	8	8	8	1	1	1	1	1	1	1	1	1
8E/9	8	8	8	8	8	8	8	8	8	1	1	2	1	1	3	1	1	4
7E/9	8	8	5	8	8	6	8	8	7	1	1	2	1	1	3	1	1	4
2E/3	8	8	5	8	8	6	8	8	7	1	2	2	1	3	3	1	4	4
5E/9	8	5	5	8	6	6	8	7	7	1	2	2	1	3	3	1	4	4
4E/9	8	5	5	8	6	6	8	7	7	2	2	2	3	3	3	4	4	4
E/3	5	5	5	6	6	6	7	7	7	2	2	2	3	3	3	4	4	4
2E/9	5	5	5	6	6	6	7	7	7	5	2	2	6	3	3	7	4	4
E/9	6	6	2	5	5	3	7	7	4	5	2	2	6	3	3	7	4	4
0	6	6	2	5	5	3	7	7	4	5	5	2	6	6	3	7	7	4
-E/9	6	2	2	5	3	3	7	4	4	5	5	2	6	6	3	7	7	4
-2E/9	6	2	2	5	3	3	7	4	4	5	5	5	6	6	6	7	7	7
-E/3	2	2	2	3	3	3	4	4	4	5	5	5	6	6	6	7	7	7
-4E/9	2	2	2	3	3	3	4	4	4	8	5	5	8	6	6	8	7	7
-5E/9	1	2	2	1	3	3	1	4	4	8	5	5	8	6	6	8	7	7
-2E/3	1	2	2	1	3	3	1	4	4	8	8	5	8	8	6	8	8	7
-7E/9	1	1	2	1	1	3	1	1	4	8	8	5	8	8	6	8	8	7
-8E/9	1	1	2	1	1	3	1	1	4	8	8	8	8	8	8	8	8	8
-E	1	1	1	1	1	1	1	1	1	8	8	8	8	8	8	8	8	8

Table.2 Direct Control Algorithm